J. Chem. Sci. (2020)132:132
https://doi.org/10.1007/s12039-020-01831-z

REGULAR ARTICLE

Role of the solvent medium in the wet-chemical synthesis of $CuSbS_2$, Cu_3SbS_3, and bismuth substituted Cu_3SbS_3

SHALU ATRI, MEENAKSHI GUSAIN, PRASHANT KUMAR, SITHARAMAN UMA and RAJAMANI NAGARAJAN*

Materials Chemistry Group, Department of Chemistry, University of Delhi, Delhi 110 007, India
E-mail: rnagarajan@chemistry.du.ac.in; shaluatri1992@gmail.com; meenuscorpio20@gmail.com; prashantpraveen12@gmail.com; suma@chemistry.du.ac.in

MS received 14 February 2020; revised 13 July 2020; accepted 20 July 2020

Abstract. Co-thermal decompositions of equimolar concentrations of thiourea complexes ($[Cu(tu)_3]Cl$ and $[Sb(tu)_2]Cl_3$) in ethylene glycol and ethanolamine were attempted. Based on the results from powder X-ray diffraction, Raman spectroscopy, and energy dispersive spectral analysis of the products, Cu_3SbS_3 in cubic symmetry emerged from ethylene glycol. In contrast, orthorhombic $CuSbS_2$ resulted from the ethanolamine medium. The generation of copper-rich and copper-poor sulfides was found to be the major reason behind the formation of these stoichiometries of the Cu-Sb-S system as verified by reacting the preformed Cu-S and Sb-S species in ethanolamine and ethylene glycol. Attempts to include bismuth (up to 50 mol%) for antimony were successful only in ethylene glycol medium. The inclusion of bismuth stabilized the orthorhombic form of Cu_3SbS_3, possibly due to the non-bonded lone pairs present on Bi^{3+} and Sb^{3+}-ions. The inclusion of bismuth confirmed from the successful refinement of powder X-ray diffraction pattern by the Rietveld method, Raman spectroscopy, and energy dispersive spectroscopy analysis. $CuSbS_2$, Cu_3SbS_3 (cubic) and $Cu_3Sb_{0.50}Bi_{0.50}S_3$ showed broad absorption extending up to visible region in their UV-visible spectra. The bandgap values of 1.31, 1.40 and 0.94 eV were estimated by Tauc plots for Cu_3SbS_3, $CuSbS_2$, and $Cu_3Sb_{0.50}Bi_{0.50}S_3$, respectively.

Keywords. Powders; Chemical preparation; X-ray methods; Optical properties.

1. Introduction

The recent trends in research are directed towards the development of renewable energy sources. There are specific efforts to recover industrial and automobile waste heat and convert them into electricity. The thermoelectric generators, capable of converting waste heat to power, consist of p-type and n-type semiconducting elements/compounds. Copper-based chalcogenides are promising semiconductor materials exhibiting applications in the energy sector as photovoltaic, thermoelectric, supercapacitor, dye-sensitized solar cells, and as electrodes in batteries.[1–5] For sustainable solar cell materials, copper antimony/bismuth sulfides have superseded copper indium sulfide or copper gallium sulfide from many aspects, including cost-effective nature, non-toxicity, and earth abundance. $CuSbS_2$ (Chalcostibite), $Cu_{12}Sb_4S_{13}$ (Tetrahedrite), Cu_3SbS_3 (Skinnerite), and Cu_3SbS_4 (Fematinite) are the four accessible ternary phases which are inherently p-type semiconductors (due to dominant copper vacancy).[6,7] Their bandgaps lie in the range 0.5–2.0 eV with absorption coefficient values over 10^5 cm^{-1}.[8] $CuSbS_2$ is relatively less explored and structurally very different than $CuInS_2$ due to low valence state of antimony with stereochemically active lone pair of electrons leading to lowering of its symmetry to orthorhombic (space group *Pnma)*. In the structure of $CuSbS_2$, copper atoms form a regular tetrahedral network with sulfur. In contrast, the antimony is forming 5-fold coordination with sulfur in a distorted square-based pyramid arrangement (SbS_5).[9] Cu_3SbS_3 (skinnerite) shows temperature-dependent polymorphism involving the mobility of Cu atoms

*For correspondence

Electronic supplementary material: The online version of this article (https://doi.org/10.1007/s12039-020-01831-z) contains supplementary material, which is available to authorized users.

Published online: 25 September 2020

among the available crystallographic positions.[10,11] Below 263 K, Cu_3SbS_3 possesses a wittichenite-type orthorhombic structure (S.G. $P2_12_12_1$), where Sb is threefold coordinated with three S atoms as SbS_3 pyramidal unit. The Cu atoms coordinated with three S atoms in a distorted trigonal plane. The existence of a very narrow thermodynamic stability of the compositions of the Cu-Sb-S system makes their synthesis quite challenging by the conventional method of reacting the constituents in elemental form, pushing researchers to explore alternate routes of making these compositions in pure form.[6,12–22] The arrival of nanoscience and the subsequent technological consequences is a boon for chemical solution-based synthesis by which one can effectively control the nucleation and the kinetics of growth of crystalline materials.[12–15] The downside of such procedures is the use of excessive amounts of long-chain surfactants and environment unfriendly solvents. The careful selection of metal and sulfide precursors and experimental conditions play a pivotal role in stabilizing a particular stoichiometry in a desired morphology and shape.[8,16–23] Additionally, the reaction controls, including the reaction temperature, precursor type, the molar ratio of reactants, and the ligand composition, determine the phase purity of compositions belonging to the Cu-Sb-S system.[8,16–23] Limited exploration of wet-chemical methods exists for the bulk synthesis of copper bismuth sulfides as well.[24–27] Among many compositions reported in the Cu-Bi-S system, Cu_3BiS_3 possesses optical properties (bandgap of about 1.5 eV and optical absorption co-efficient of $\alpha > 10^4$ cm^{-1}) that are quite ideal to be used as an absorber layer in photoelectric applications.[24–27] The complications of synthesizing compositions of the Cu-Bi-S system are quite similar to that of the Cu-Sb-S system. It is therefore highly desirable to devise a robust wet-chemical method involving environment-friendly solvents to synthesize compositions of the Cu-Sb-S system. Also, such a technique should be rapid and highly reproducible. With these objectives, the current study is undertaken in which simple co-thermal decomposition of thiourea precursors of copper and antimony ($[Cu(tu)_3]Cl$ and $[Sb(tu)_2]Cl_3$) is carried out in a defined 1:1 molar ratio in solvents (ethylene glycol and ethanolamine) whose boiling points are closer to each other. Further, we attempted the substitution of Bi^{3+} for Sb^{3+} in Cu_3SbS_3, which stabilized the orthorhombic polymorphic modification of Cu_3SbS_3. The inclusion of bismuth for antimony also brought changes in optical absorption characteristics. The results of this study are discussed in the succeeding sections.

2. Experimental

2.1 *Synthesis of metal-thiourea complexes*

$CuCl_2{\cdot}2H_2O$ (Merck, 99.0%), Bi_2O_3 (Sigma Aldrich, 99.9%), Sb_2O_3 (Sigma Aldrich, 99.9 + %), Na_2SO_3 (SRL, 98.0%) and thiourea (Merck, 99.0%) were used as the starting materials to generate the metal-thiourea complexes. $[Cu(tu)_3]Cl$ complex was prepared following an established procedure.[28] 0.099 g (1 mmol) of freshly prepared CuCl was dissolved in 5 mL aqueous solution of thiourea (0.228 g, 3 mmol) stepwise under constant stirring for 30 min, followed by filtration and recrystallization. Similarly, antimony trichloride solution generated in situ from the reaction of 1.457 g of Sb_2O_3 in 20 mL of HCl (5 M) was added to ten milliliters of aqueous thiourea (1.522 g).[29] The mixture was stirred vigorously at room temperature for nearly three hours and was transferred to a petri dish. A free-flowing complex was isolated after drying. It was dried naturally. Similarly, $[Bi_3(tu)_3]Cl_3$ was prepared by reacting to a 20 mL solution of 5 M HCl containing 2.329 g of Bi_2O_3 and a 10 mL aqueous solution containing 1.522 g of thiourea.[30]

2.2 *Synthesis of mixed metal sulfides*

0.327 g (1 mmol) of $[Cu(tu)_3]Cl$ and 0.380 g (1 mmol) of $[Sb(tu)_2]Cl_3$ were refluxed in 60 mL of ethanolamine (Merck > 99%) for 90 min. The product, after the reaction, was separated by filtration and washed with double distilled water followed by ethanol and carbon disulfide. The co-thermal decomposition of copper and antimony complexes in a 1:1 molar ratio was also carried out in ethylene glycol (Merck > 99.5%) under refluxing conditions for 90 min. For 50 mol % substitution of bismuth in Cu-Sb-S system; 0.982 g (3.00 mmol) of $[Cu(tu)_3]Cl$, 0.190 g (0.50 mmol) of $[Sb(tu)_2]Cl_3$ and 0.131 g (0.167 mmol) of $[Bi_3(tu)_3]Cl_3$ were mixed well in a pestle and mortar and added to 60 mL of ethylene glycol. A black colored product emerged on refluxing for six hours was separated by centrifugation. The products were washed repeatedly with double distilled water, ethanol, and carbon disulfide.

2.3 *Characterization*

High-resolution X'Pert PANanalytical diffractometer, equipped with a Xe proportional detector employing Cu Kα radiation (λ = 1.5418 Å), was employed to collect the powder X-ray diffraction (PXRD) patterns. Refinements of lattice parameters and structure were performed by the Le Bail and Rietveld method using the TOPAS 3 and GSAS + EXPGUI program.[31–33] Fourier transformed infrared (FTIR) spectra were gathered using a Perkin Elmer 2000 spectrometer using KBr disks. Raman spectra of samples in pellet form were obtained using a Renishaw *via*

Microscope system with a diode laser (λ = 785 nm). The thermal analysis of metal-thiourea precursors were analyzed using a NETZSCH STA-449 F3 instrument in the temperature range of 30-700 °C at a heating rate of 10 °C/min. Morphology examination and qualitative analysis of the elements in the samples were carried out by scanning electron microscopy (SEM) and by energy dispersive spectral analysis (EDS) using JEOL 6610 LV microscope. UV-visible spectra of the samples were recorded using a Perkin-Elmer Lambda 35 scanning double-beam spectrometer.

3. Results and Discussion

In metal-thiourea complexes, thiourea plays a dual role of complexing with the metal ion as well as the source of sulfur. Thiourea complexes, in general, dissociate at moderate temperatures and get easily solubilized in solvent media, which in turn increases the rate of reaction. During the dissociation of metal-thiourea precursors, generation of S^{2-} ions occurs according to the following equation:

$$NH_2CSNH_2 + H_2O \rightarrow H_2S + CO_2 + NH_3$$

As this reaction involves the liberation of gaseous CO_2, the products will be porous and crystalline.[34,35] The white color complex resulted from the reaction of CuCl, and thiourea was analyzed with the help of FTIR, Raman spectra, and thermal analysis techniques (Figure S1, Supplementary Information). The spectral features match well with the data available for $[Cu(tu)_3]Cl$.[28] The sample loses a significant portion of the ligand by 300 °C as revealed by its thermogram. The FTIR, Raman spectra, and thermal analysis of the light yellow color complex from the reaction of antimony chloride and thiourea resemble closely with the features reported for $[Sb(tu)_2]Cl_3$ (Figure S2, Supplementary Information).[29]

Figure 1 shows the PXRD patterns of the products from the reaction of thiourea complexes of copper and antimony ($[Cu(tu)_3]Cl$ and $[Sb(tu)_2]Cl_3$) in a 1:1 molar ratio in ethanolamine and ethylene glycol individually under refluxing conditions. While $CuSbS_2$ is formed from the reaction conducted in ethanolamine, Cu_3SbS_3 forms when the solvent medium changed to ethylene glycol (Figure 1(a) and (b)). Both these compositions have crystallites with near-spherical morphology in their SEM images (Figure 1(a) and (b)). The existence of copper, antimony, and sulfur in 1: 1: 2 and 3:1:3 ratios, is revealed by energy dispersive spectral analysis (Figure 1(a) and (b)).

Successful refinement of the PXRD pattern of $CuSbS_2$ in the *Pnma* space group by the Le Bail method

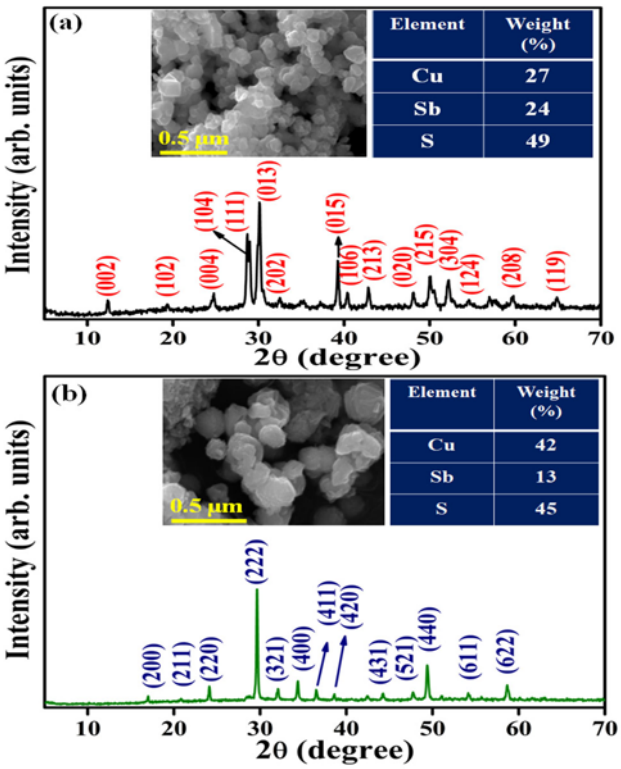

Figure 1. Shows PXRD patterns of the products from the refluxing reaction of $[Cu(tu)_3]Cl$ and $[Sb(tu)_2]Cl_3$ complexes in 1:1 molar ratio in (**a**) ethanolamine and (**b**) ethylene glycol for 90 min. Insets show SEM image, energy dispersive spectral analysis.

yields lattice dimensions of a = 6.0240 (8), b = 3.8005 (5), and c = 14.508 (2) Å (Figure 2(a)). In the Raman spectrum, $CuSbS_2$ shows only one band at 335 cm^{-1}, which corresponds to Sb-S stretching vibrations (Figure 2(a)). The unit-cell dimension of 10.428 (7) Å is deduced from the successful refinement of the PXRD pattern of Cu_3SbS_3 in the *I-43 m* space group by the Le Bail method (Figure 2(b)). Cu_3SbS_3 shows two characteristic bands at 321 and 353 cm^{-1} in its Raman spectrum at room temperature (Figure 2(b)).[36]

Generally, reaction parameters such as temperature, duration of reaction, and nature of the sulfur precursor have been used to control the size and morphology of the nanocrystals of Cu-Sb-S compositions.[8,16–23] Employing 1-octadecene (a high boiling solvent), $CuSbS_2$ nanocrystals have been made beginning either from the equimolar ratio of copper and antimony or 3:1 molar ratio of copper and antimony.[8,16–23] Our trials on the co-thermal decomposition of thiourea precursors of copper and antimony (in 1:1 molar ratio) at 150 and 300 °C for 90 min yielded $CuSbS_2$ in orthorhombic symmetry (Figure S3, Supplementary Information). There were additional reflections due to Cu_2S (tetragonal and hexagonal) in the PXRD

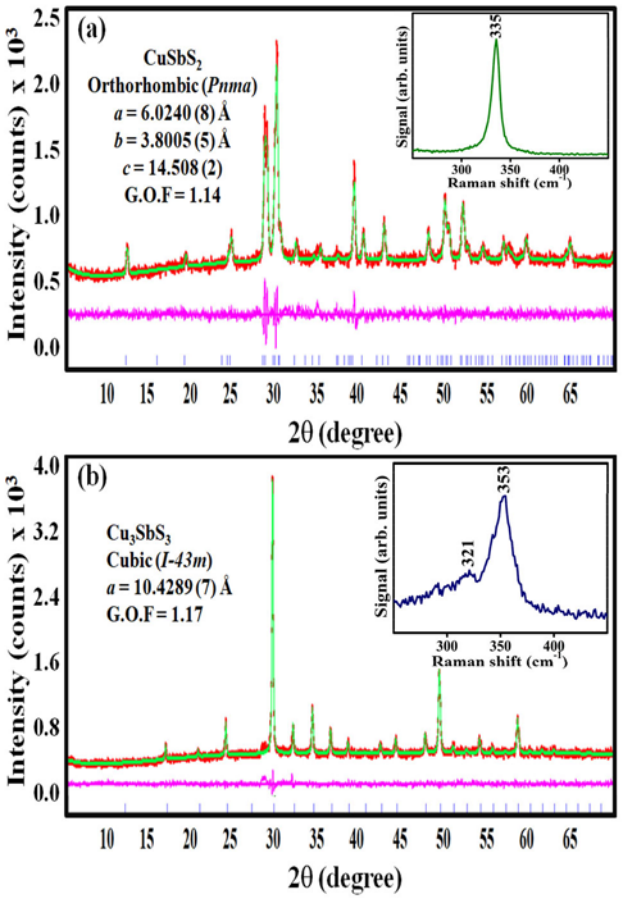

Figure 2. Shows Le Bail refinement of PXRD patterns of (**a**) $CuSbS_2$ and (**b**) Cu_3SbS_3 (Redline-experimental data; green line-calculated profile; pink line-difference profile. Vertical bars indicate Bragg positions). Inset shows their room temperature Raman spectra.

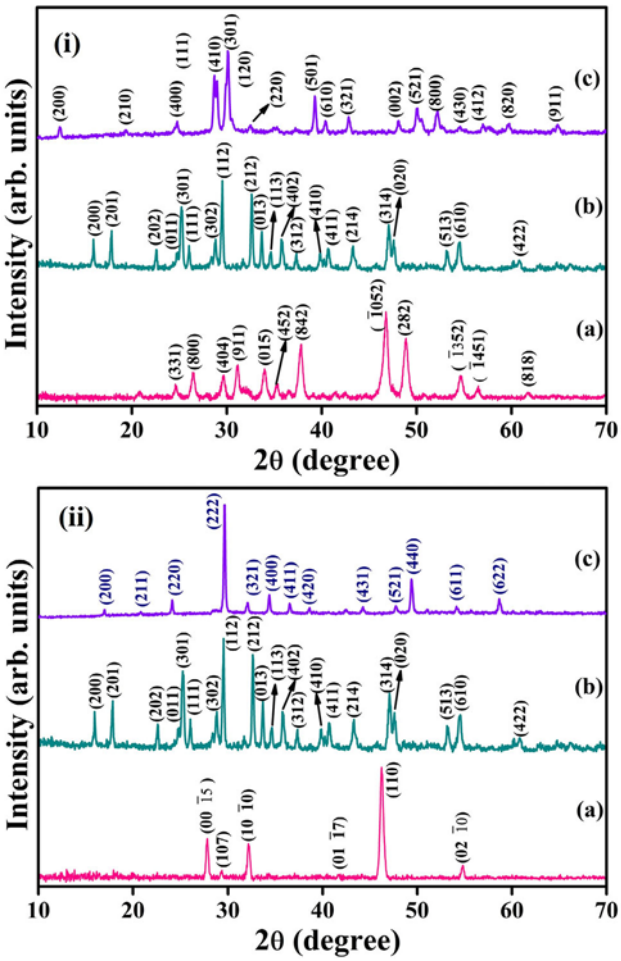

Figure 3. (i) Shows the PXRD pattern of the product from the refluxing reaction of (**a**) $[Cu(tu)_3]Cl$ in ethanolamine, (**b**) $[Sb(tu)_2]Cl_3$ in ethanolamine and (c) the product obtained by mixing hot colloidal suspensions containing Cu-S species and Sb-S species in ethanolamine. In (ii), the PXRD pattern of the product from the refluxing reaction of (**a**) $[Cu(tu)_3]Cl$ in ethylene glycol, (**b**) $[Sb(tu)_2]Cl_3$ in ethylene glycol, and (**c**) the product obtained by mixing hot colloidal suspensions containing Cu-S species and Sb-S species in ethylene glycol are shown.

patterns. The realization of $CuSbS_2$ in ethanolamine medium (a low boiling solvent) hints that its formation can not be explained by the refluxing conditions alone. Sb_2S_3 can be the only stable phase from the thermal decomposition of $[Sb(tu)_2]Cl_3$ complex. However, this is not the case in the case of copper sulfides. Depending on the nature of the solvent, copper-rich and copper-deficient sulfides can be formed from the decomposition of $[Cu(tu)_3]Cl$. When we dissociated $[Cu(tu)_3]Cl$ in four different solvents viz., ethylene glycol, ethanolamine, ethylenediamine, and 1, 2-ethanedithiol, in which a systematic variation of the functional groups on both sides of the $-CH_2-CH_2-$ chain was present, we found an interesting variation of the nature of the copper sulfide. The powder X-ray diffraction patterns of the products from the dissociation of $[Cu(tu)_3]Cl$ in ethylene glycol, 1, 2-ethanedithiol, ethanolamine, and ethylenediamine under refluxing conditions for 90 min are presented in Figure S4 (Supplementary Information). The chosen solvents are bidentate chelate in which the metal-thiourea precursors will be less stable under refluxing conditions yielding metal sulfides. All the observed reflections in the powder X-ray diffraction of the product, obtained using ethylene glycol, match very well with the hexagonal Cu_9S_5 ($Cu_{1.8}S$) (dignite) phase with the JCPDS File No. 47-1748 (Figure S4(a), Supplementary Information). The same product results when 1, 2-ethanedithiol in which the OH-groups in ethylene glycol are replaced with SH-groups (Figure S4(b), Supplementary Information).

The dissociated products from both the ethanolamine and ethylenediamine show more reflections in the powder X-ray diffraction patterns as compared to the ones from ethylene glycol and 1, 2-ethanedithiol,

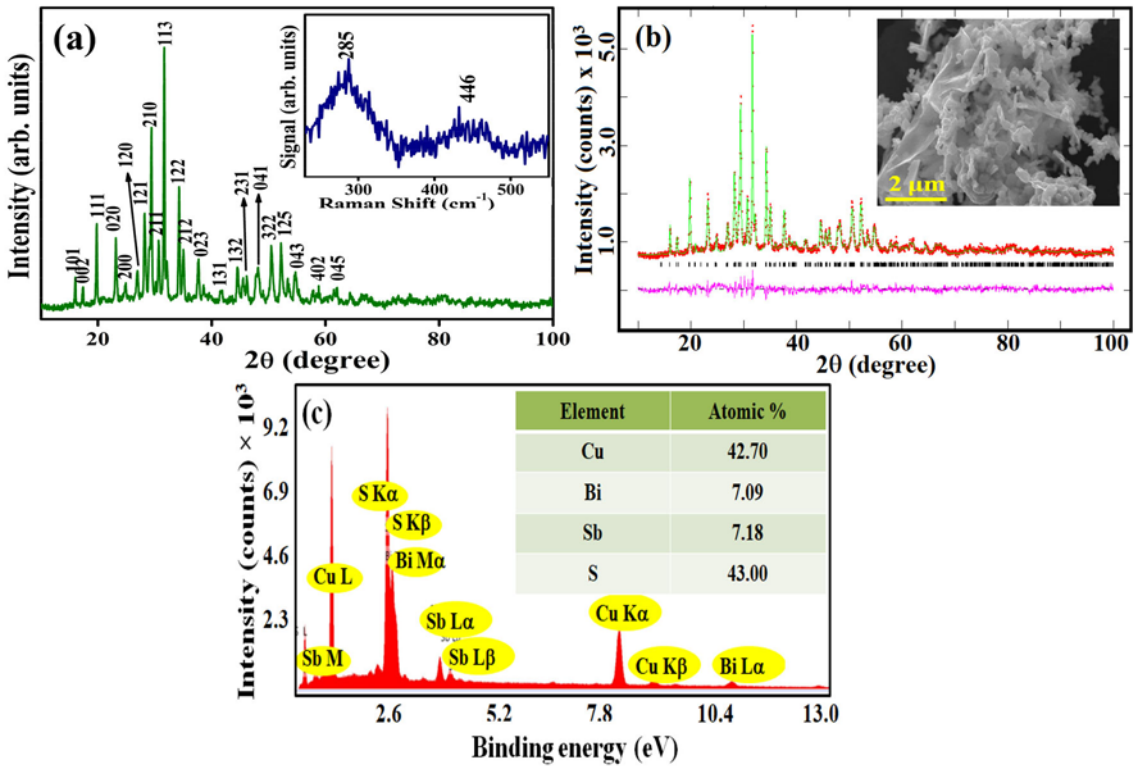

Figure 4. (**a**) and (**b**) show PXRD pattern of the product from the refluxing reaction of $[Cu(tu)_3]Cl$, $[Sb(tu)_2]Cl_3$, and $[Bi_3(tu)_3]Cl_3$ complexes in ethylene glycol and its refinement by the Rietveld method (redline-experimental data; green line-calculated profile; pink line-difference profile; vertical bars-Bragg positions). (**c**) Shows the energy dispersive spectrum of the sample. Insets in (**a**), (**b**), and (**c**) show the Raman spectrum, SEM image, and elemental analysis of $Cu_3Sb_{0.50}Bi_{0.50}S_3$ sample.

Table 1. Crystallographic (PXRD) parameters of $Cu_3Sb_{0.50}Bi_{0.50}S_3$.

Crystal system	Orthorhombic
Space group	$P2_12_12_1$
Lattice constants:	
a (Å)	6.621 (5)
b (Å)	7.699 (7)
c (Å)	10.272 (6)
Cell volume (Å^3)	523.73 (5)
Formula weight	612.2
Z	4
Density (calc.)	5.823 g cm^{-3}
Radiation	CuK_α
2θ range	10–100°
No. of data points	2249
Agreement factors:	
R_p	0.0491
R_{wp}	0.0386
χ^2	4.361

indicating their lower symmetry (Figure S4(c) and (d), Supplementary Information). While all the reflections in the powder X-ray diffraction pattern of the product from ethylenediamine correspond to a monoclinic Cu_2S (JCPDS-File No. 83-1462), the product, from the reaction using ethanolamine, shows a very close match with the monoclinic $Cu_{31}S_{16}$ ($Cu_{1.93}S$) in its PXRD pattern (JCPDS-File No. 34-0660). Despite their boiling points being closer, the stabilized Cu-Sb-S stoichiometry product from ethylene glycol and ethanolamine are different, suggesting additional factors, other than the thermal effects, were responsible for their formation.

We believe the formation mechanism of $CuSbS_2$ and Cu_3SbS_3 may involve the insertion of antimony into the copper-rich or copper poor sulfide as seed crystal as per the following reaction:[18,19]

$$Cu_{2-x}S + Sb_2S_3 \rightarrow Cu\text{-}SbS$$

The Cu-S species generated after refluxing the $[Cu(tu)_3]Cl$ in ethanolamine for 45 min was added to Sb-S species generated (from $[Sb(tu)_2]Cl_3$) under similar conditions and refluxed further for 90 min to examine the nature of the product. The PXRD pattern from this trial is presented in Figure 3(i) in which the intensity and the position of diffracted peaks match well with orthorhombic $CuSbS_2$. A similar exercise

Table 2. Presents positional, occupancies, and thermal parameters of $Cu_3Sb_{0.50}Bi_{0.50}S_3$.

Atoms	*Wyck position*	*x/a*	*y/b*	*Z/c*	S.O. F	U(iso)Å^2
Sb1	4a	0.6290(5)	0.3011(5)	0.2444(7)	0.53(2)	0.0203(16)
Bi2	4a	0.6290(5)	0.3011(5)	0.2444(7)	0.47(2)	0.0203(16)
Cu3	4a	0.0401(21)	0.5532(14)	0.0305(9)	1	0.045(5)
Cu4	4a	0.0663(16)	0.1955(13)	0.1031(10)	1	0.045(5)
Cu5	4a	0.1406(17)	0.3514(14)	0.4006(9)	1	0.054(5)
S6	4a	0.4084(34)	0.1720(25)	0.0603(18)	1	0.010(6)
S7	4a	0.4356(28)	0.1912(23)	0.4250(17)	1	0.052(8)
S8	4a	0.1029(30)	0.5474(20)	0.2587(25)	1	0.044(6)

Table 3. Lists the summary of selected bond distances in the crystal structure of $Cu_3Bi_{0.50}Sb_{0.50}S_3$.

Atoms	Interatomic distances (Å)
Sb1/Bi2–S7	2.4081(1) × 1
Sb1/Bi2–S6	2.5878 (1) × 1
Sb1/Bi2–S8	2.6391 (2) × 1
Cu3–S6	2.1532(1) × 1
Cu3–S7	2.2528(2) × 1
Cu3–S8	2.3816(1) × 1
Cu4–S8	2.1380(1) × 1
Cu4–S6	2.2251(1) × 1
Cu4–S6	2.3146(2) × 1
Cu5–S8	2.1129(1) × 1
Cu5–S7	2.2729(1) × 1
Cu5–S7	2.3235(1) × 1

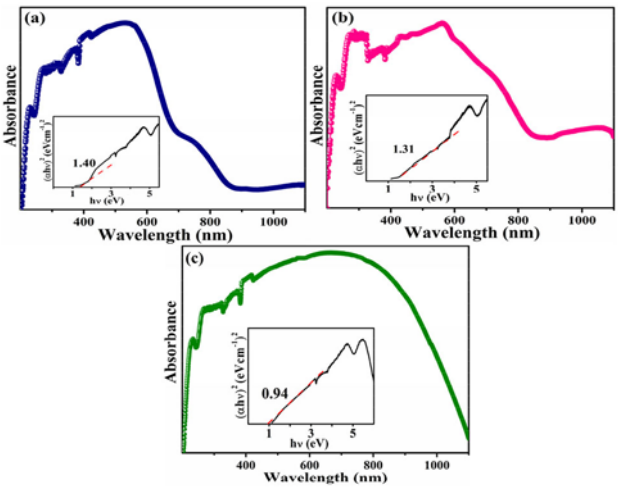

Figure 5. Shows UV-visible spectra of (**a**) $CuSbS_2$, (**b**) Cu_3SbS_3 and (**c**) $Cu_3Sb_{0.50}Bi_{0.50}S_3$, respectively. Insets show the corresponding Tauc plots for bandgap calculation.

was undertaken by changing the solvent medium from ethanolamine to ethylene glycol in which the formation of cubic Cu_3SbS_3 was noticed (Figure 3(ii)). These results validated our hypothesis that copper-rich and copper-poor sulfides were responsible for the formation of $CuSbS_2$ and Cu_3SbS_3 in ethanolamine and ethylene glycol solvent mediums, respectively.

We explored this synthesis approach to generate bismuth-containing quaternary sulfides (Cu-Sb-Bi-S) as such substitutions have been reported to enhance the thermoelectric property of Cu_3SbS_3 system.[37] While the attempts to prepare a quaternary sulfide with bismuth are not successful in ethanolamine, the reaction in ethylene glycol produces a black colored product whose PXRD pattern is indexable in orthorhombic symmetry with space group $P2_12_12_1$ having lattice parameters of $a = 6.6213$ (5), $b = 7.6990$ (7) and $c = 10.2728$ (6) Å (Figure 4(a) and (b)).[38,39]

The refinement of PXRD patterns of $Cu_3Sb_{0.50}Bi_{0.50}S_3$ (considering orthorhombic Cu_3SbS_3 (S.G. $P2_12_12_1$) as the structural model) by the Rietveld method is successful (Figure 4(b)).[38–40] The inclusion of bismuth in place of antimony expands the unit cell parameters due to the larger ionic radius of Bi^{3+} as compared with Sb^{3+}. From the refined occupancies, nearly equal concentrations of bismuth and antimony are evident (Tables 1 and 2). It is noteworthy that the inclusion of bismuth for antimony stabilized the orthorhombic polymorph of Cu_3SbS_3, quite similar to the stabilization of cubic Cu_3SbS_4 by iron substitution.[40] The critical bond distances of this structure from the final cycle of the refinement of the PXRD pattern by the Rietveld method are collected in Table 3. The Raman spectrum of the Cu-Sb-Bi-S sample shows a similarity with the features reported for Cu_3SbS_3 in orthorhombic symmetry (inset of Figure 4(a)).[41,42] The band centered at $\sim$ 446 cm^{-1} is quite typical of Cu_3SbS_3 in orthorhombic symmetry.[41,42] The combined vibrations involving Cu-S and Sb-S units of the crystal structure manifest at 285 cm^{-1} (Figure 4(a)).[38,39] The EDS analysis carried out on the SEM image of the sample confirms the stoichiometry of Cu, Sb, Bi, and S to be 3: 0.50: 0.50: 3 (Figure 4(c)).

$CuSbS_2$, Cu_3SbS_3 (cubic) and $Cu_3Sb_{0.50}Bi_{0.50}S_3$ (orthorhombic) show absorption extending up to

visible region in their UV-visible spectra (Figure 5). From the Tauc plot ($(\alpha h\upsilon)^2$ versus photon energy (eV)), optical bandgap values of 1.40, 1.31 and 0.94 eV are estimated for $CuSbS_2$, Cu_3SbS_3 and $Cu_3Sb_{0.50}Bi_{0.50}S_3$, respectively (Figure 5). They are close to the optical bandgap values reported in the literature.[8] The inclusion of bismuth brought down the bandgap considerably.

4. Conclusions

The use of air-stable precursors, simplicity of operation, scalable possibility, one pot, and shorter reaction duration to generate monophasic products are the striking advantages of the current work. The formation of $CuSbS_2$ and Cu_3SbS_3 in ethanolamine and ethylene glycol respectively is reasoned out to relate with the nature of copper sulfide (copper-rich and copper-poor) from $[Cu(tu)_3]Cl$ as seed crystals. The formation of quaternary sulfide, $Cu_3Sb_{0.50}Bi_{0.50}S_3$, was feasible in ethylene glycol as a solvent medium, promoted by the additional factor of its high viscosity facilitating higher miscibility. Interestingly, such a substitution stabilized Cu_3SbS_3 in orthorhombic symmetry, similar to the stabilization of cubic Cu_3SbS_4 by iron substitution.[40]

Supplementary Information (SI)

Figures S1-S4 are available at www.ias.ac.in/chemsci.

Acknowledgments

Financial support from SERB (EMR/2016/006131 and EMR/2016/006762) Government of India for this work is gratefully acknowledged. Shalu thanks UGC, Govt. of India, for the research fellowship.

References

1. Welch A W, Baranowski L L, Zawadzki P, De Hart C, Johnston S, Lany S, Wolden C A and Zakutayev A 2016 Accelerated development of $CuSbS_2$ thin-film photovoltaic device prototypes *Prog. Photovolt. Res. Appl.* **24** 929
2. Gudelli V K, Kanchana V, Vaitheeswaran G, Svane A and Christensen N E 2013 Thermoelectric properties of chalcopyrite type $CuGaTe_2$ and chalcostibite $CuSbS_2$ *J. Appl. Phys.* **114** 223707
3. Ramasamy K, Gupta R K, Sims H, Palchoudhury S, Ivanov S and Gupta A 2015 Layered ternary sulfide $CuSbS_2$ nanoplates for flexible solid-state supercapacitors *J. Mater. Chem. A* **3** 13263
4. Choi Y C, Yeom E J, Ahn T K and IlSeok S 2015 $CuSbS_2$-sensitized inorganic-organic heterojunction solar cells fabricated using a metal-thiourea complex solution *Angew. Chem. Int. Ed.* **54** 4005
5. Marino C, Block T, Pottgen R and Villevieille C 2017 $CuSbS_2$ as a negative electrode material for sodium-ion batteries *J. Power Sources* **342** 616
6. Skinner B J, Luce F D and Makovicky E 1972 Studies of the sulfosalts of copper III; Phases and phase relations in the system Cu-Sb-S *Econ. Geol.* **67** 924
7. Bryndzia L T and Kleppa O J 1988 High-temperature reaction calorimetry of solid and liquid phases in part of the quasi-binary system Cu_2S-Sb_2S_3 *Am. Mineral.* **73** 707
8. Ramasamy K, Sims H, Butler W H and Gupta A 2014 Selective nanocrystal synthesis and calculated electronic structure of all four phases of copper-antimony-sulfide *Chem. Mater.* **26** 2891
9. Kyono A and Kimata M 2005 Crystal structures of chalcostibite ($CuSbS_2$) emplectite ($CuBiS_2$): Structural relationship of stereochemical activity between chalcostibite and emplectite *Am. Mineral.* **90** 162
10. Whitfield H J 1980 Polymorphism in skinnerite *Solid State Commun.* **33** 747
11. Pfitzner A 1998 Disorder of Cu^+ in Cu_3SbS_3: Structural investigations of the high- and low-temperature modification *Z. Kristallogr.* **213** 228
12. C N R Rao, H C Mult, A Müller and A K Cheetham 2007 (Eds.) *Nanomaterials chemistry: Recent developments and new directions* (Wiley-VCH Verlag GmbH & Co.)
13. Rodriguez R, Hendricks M P, Cossairt B, Liu H and Owen J S 2013 Conversion reactions of cadmium chalcogenide nanocrystal precursors *Chem. Mater.* **25** 1233
14. Mourdikoudis S and Liz-Marzan L M 2013 Oleylamine in nanoparticle synthesis *Chem. Mater.* **25** 1465
15. Jun YW, Choi J S and Cheon J 2006 Shape control of semiconductor and metal oxide nanocrystals through nonhydrolytic colloidal routes *Angew. Chem. Int. Ed.* **45** 3414
16. Ramasamy K, Sims H, Butler W H and Gupta A 2014 Mono-, Few-, and multiple layers of copper antimony sulfide ($CuSbS_2$): A ternary layered sulfide *J. Am. Chem. Soc.* **136** 1587
17. Yang B, Wang L, Han J, Zhou Y, Song H, Chen S, Zhong J, Lv L, Niu D and Tang J 2014 $CuSbS_2$ as a promising earth-abundant photovoltaic absorber material: A combined theoretical and experimental study *Chem. Mater.* **26** 3135
18. Liang Q, Huang K, Ren X, Zhang W, Xie R and Feng S 2016 Synthesis of Cu-Sb-S nanocrystals: Insight into the mechanism of composition and crystal phase selection *CrystEngComm* **18** 3703
19. Zou Y and Jiang J 2014 Colloidal synthesis of chalcostibite copper antimony sulfide nanocrystals *Mater. Lett.* **123** 66
20. Yan C, Su Z, Gu E, Cao T, Yang J, Liu J, Liu F, Lai Y, Li J and Liu Y 2012 Solution-based synthesis of chalcostibite ($CuSbS_2$) nano bricks for solar energy conversion *RSC Adv.* **2** 10481

21. Moosakhani S, Alvani A A S, Mohammadpour R, Ge Y and Hannula S P 2018 Solution synthesis of $CuSbS_2$ nanocrystals: A new approach to control shape and size *J. Alloys Compd.* **736** 190
22. Hobbis D, Wei K, Wang H, Martin J and Nolas G S 2017 Synthesis, structure, Te alloying, and physical properties of $CuSbS_2$ *Inorg. Chem.* **56** 14040
23. Jiasong Z, Weidong X, Huaidong J, Wen C, Lijun L, Xinyu Y, Xiaojuan L and Haitao L 2010 A simple L-cystine-assisted solvothermal approach to Cu_3SbS_3 nanorods *Mater. Lett.* **64** 1499
24. Gerein N J and Haber J A 2006 One-step synthesis and optical and electrical properties of thin-film Cu_3BiS_3 for use as a solar absorber in photovoltaic devices *Chem. Mater.* **18** 6297
25. Chakraborty M, Thangavel R, Komninou P, Zhou Z and Gupta A 2019 Nanospheres and nanoflowers of copper bismuth sulfide (Cu_3BiS_3): Colloidal synthesis, structural, optical, and electrical characterization *J. Alloys Compd.* **776** 142
26. Viezbicke BD and Birnie D P 2013 Solvothermal synthesis of Cu_3BiS_3 enabled by precursor complexing *ACS Sustain. Chem. Eng.* **1** 306
27. Zhong J, Xiang W, Cai Q and Liang X 2012 Synthesis, characterization and optical properties of flower-like Cu_3BiS_3 nanorods. *Mater. Lett.* **70** 63
28. Bombicz P, Mutikainen I, Krunks M, Leskela T, Madarasz J and Niinisto L 2004 Synthesis, vibrational spectra and X-ray structures of copper (I) thiourea complexes *Inorg. Chim. Acta* **357** 513
29. Ozturk II, Kourkoumelis N, Hadjikakou S K, Manos M J, Tasiopoulos A J, Butler I S, Balzarini J and Hadjiliadis N 2011 Interaction of antimony (III) chloride with thiourea, 2-mercapto-5-methyl-benzimidazole, 3-methyl-2-mercaptobenzothiazole, 2-mercaptopyrimidine, and 2-mercaptopyridine *J. Coord. Chem.* **64** 3859
30. Sankar R, Raghavan C M and Jayavel R 2007 Bulk growth and characterization of semi-organic nonlinear optical bis thiourea bismuth chloride single crystals *Cryst. Growth Des.* **7** 501
31. Coelho A A 2003 TOPAS Version 3.1, Bruker AXS GmbH, Karlsruhe, Germany
32. Larson A-C and Von Dreele R B 2004 General Structure Analysis System (GSAS), Los Alamos National Laboratory Report LAUR **86** 748
33. Toby B H 2001 EXPGUI, A Graphical User Interface for GSAS *J. Appl. Crystallogr.* **34** 210
34. Kumar P, Gusain M and Nagarajan R 2011 Synthesis of $Cu_{1.8}S$ and CuS from copper-thiourea containing precursors; Anionic (Cl^-, NO_3^-, SO_4^{2-}) influence on the product stoichiometry *Inorg. Chem.* **50** 3065
35. Gorai S, Ganguli D and Chaudhuri S 2005 Synthesis of copper sulfides of varying morphologies and stoichiometries controlled by chelating and nonchelating solvents in a solvothermal process *Cryst. Growth Des.* **5** 875
36. Qiu X, Ji S, Chen C, Liu G, Ye C 2013 Characterization, and surface-enhanced Raman scattering of near-infrared absorbing Cu_3SbS_3 nanocrystals *CrystEngComm* **15** 10431
37. Kumar D S P, Chetty R, Femi O E, Chattopadhyay K, Malar P and Mallik R C 2017 Thermoelectric properties of Bi-doped tetrahedrite *J. Electronic Mater.* **46** 2616
38. Karup-Moller S and Makovicky E 1974 Cu_3SbS_3, a new sulfosalt from the Llimaussaq alkaline intrusion South Greenland *Am. Miner.* **59** 889
39. Kocman V and Nuffield E W 1973 The crystal structure of Wittichenite, Cu_3BiS_3 *Acta Cryst. B* **29** 2528
40. Du B, Zhang R, Liu M, Chen K, Zhang H and Reece M J 2019 Crystal Structure and Improved Thermoelectric Performance of Iron Stabilized Cubic Cu_3SbS_3 - Compound *J. Mater. Chem. C* **7** 394
41. Yan C, Gu E, Liu F, Lai Y, Li J and Liu Y 2013 Colloidal synthesis and characterizations of Wittichenite copper bismuth sulfide nanocrystals *Nanoscale* **5** 1789
42. Yakushev M V, Maiello P, Raadik T, Shaw M J, Edwards P R, Krustok J, Mudryi A V, Forbes I and Martin R W 2014 Electronic and structural characterization of Cu_3BiS_3 thin films for the absorber layer of sustainable photovoltaics *Thin Solid Films* **562** 195